JOURNAL OF CATALYSIS 4, 535–545 (1965)

Reaction of Hydrogen with a Nonstoichiometric Manganese Dioxide

C. S. BROOKS

From the United Aircraft Research Laboratories
East Hartford, Connecticut

Received August 18, 1964; revised February 8, 1965

The reaction of hydrogen with a catalytically active nonstoichiometric manganese dioxide has been examined at temperatures between room temperature and 400°C employing gas chromatographic procedures. The oxidation rates for heterogeneous oxidation of hydrogen with air at concentrations below 7 vol % were found to be first order with respect to the hydrogen concentration for the temperature range 95° to 200°C. The oxidation rates for depletive oxidation of hydrogen with manganese dioxide at 1950 ppm hydrogen at 100° to 300°C were found to be first order with respect to the manganese dioxide and the data could be fitted to an equation of the form $\ln [a/(a - x)] = k''t$ where a is the initial amount of manganese dioxide present and x is the oxygen removed from the oxide lattice by hydrogen oxidation at t. The activation energy for the heterogeneous hydrogen oxidation was calculated to be 3.9 kgcal/mole compared with an activation energy of 8.7 kgcal/mole for the depletive hydrogen oxidation reaction. The activation energy for depletive hydrogen oxidation is probably enough greater than the activation energy for the heterogeneous oxidation reaction to establish that in air relatively slight demand would be made upon the lattice oxygen. The high catalytic activity and defect nature of this manganese dioxide are indicated by the amount of Mn^{3+} initially present. The oxygen of this oxide could be depleted and replenished with a high order of reversibility within the stoichiometric range of $MnO_{1.96}$ to $MnO_{1.52}$ which corresponds to the range of high activity for hydrogen oxidation.

Introduction

The effectiveness of a number of the transition metal oxides as catalysts for the heterogeneous oxidation of hydrogen and carbon monoxide has long been known, and these reactions have been investigated extensively over a period of many years. Interest in these reactions continues because their molecular simplicity makes them attractive in fundamental studies of heterogeneous catalysis and the relationship between the phenomenon of catalysis and theories of the solid state. Two specific areas of investigation involving interactions of this type are catalytic electrodes for fuel cells and the removal of oxidizable contaminants from air. The experiments described here are concerned with the kinetics of hydrogen oxidation at low temperatures (25° to 400°C) over an especially active nonstoichiometric manganese dioxide. The hydrogen oxidation rates were determined to provide a measure of the energy requirements and an insight into reaction mechanisms.

Experimental Procedure

Catalyst preparation and characterization. Forty grams of $MnCO_3$ (C.P. Fisher reagent grade) was dissolved in 65 ml of concentrated C.P. HNO_3. Seventy-five grams of $NaClO_3$ (C.P. Fisher reagent grade) was added in increments to this solution. This was thoroughly mixed and permitted to stand for 1 day with intermittent stirring. Two hundred milliliters of distilled water was added and the precipitated manganese oxide was filtered off. The filter cake was

thoroughly washed with distilled water and dried in air at 150° to 200°C. A small portion of the dried catalyst was pulverized, dispersed in acetone, and impregnated into $\frac{1}{8} \times \frac{1}{8}$-inch Al_2O_3 pellets (Norton SA 1501 catalyst carrier). The test catalyst portion consisted of 116 mg of manganese oxide supported on 11.320 g of Al_2O_3 (110°C oven dry weight basis).

The BET (*1*) nitrogen surface area of the manganese oxide catalyst supported on Al_2O_3 based on nitrogen adsorption measurements at 78°K was 0.59 (±30%) m^2/g. The manganese oxide makes the principal contribution to this area, since the specific surface area of the Al_2O_3 support was of the order of 0.005 m^2/g.

The chemical analyses of four batches of the manganese dioxide catalyst and of a reagent grade manganese dioxide (Fisher Scientific Company) are summarized in Table 1. The total manganese content was determined gravimetrically as the pyrophosphate after precipitation as manganese ammonium phosphate. Mn^{4+} was determined by dissolution in 10% aq. H_2SO_4 containing excess $Fe_2SO_4 \cdot (NH_4)_2SO_4$ and titrating the excess Fe^{2+} with standard $KMnO_4$ (Table 1). Mn^{2+} was determined from the difference between the total manganese and the Mn^{4+} analyses (Table 1). The other metal components—aluminum, chromium, copper, iron, sodium, nickel, lead, magnesium, molybdenum, silicon, and tin—were determined by emission spectrograph. The sum of all these components was less than 0.1 wt % for all five of the manganese oxides. The hydration water reported in Table 1 is the difference between the 200°C oven dry weight and the MnO_2 + MnO content of these samples. The presence of hydration water after drying at 200°C means that the water must be chemically combined with the manganese in some form such as $MnO_{2-x}(OH)_x$.

Unsupported portions of four separate batches of the active manganese dioxide catalyst preparation and a portion of reagent grade manganese dioxide were mounted in ceramic boats in a combustion furnace and heated from room temperature to 400°C in a stream of dry argon. The duration of the heating period was 60 min. The argon eluent stream was passed through Drierite weighing tubes to recover desorbed water. The final weight of the heated oxide samples was determined by removing the hot sample boat into a weighing bottle flushed with dry argon. The object of these determinations was to establish the water content after correction for the amount of oxygen lost by thermal dissociation of the oxides upon raising to a temperature of 400°C.

TABLE 1
CHEMICAL ANALYSES OF MANGANESE OXIDES

Sample	Mn Oxide	MnO_2 based on Mn^{4+} (wt %)	MnO total Mn–Mn^{4+} (wt %)	Hydration water (wt %)
Catalyst H-2-1-1	$MnO_{1.97}$	87.52	2.40	10.08
Catalyst H-2-1-2	$MnO_{1.92}$	85.96	5.68	8.36
Catalyst H-2-1-3	$MnO_{1.93}$	86.36	5.25	8.39
Catalyst H-2-1-4	$MnO_{1.97}$	85.48	1.87	12.65
Reagent grade MnO_2	$MnO_{1.99}$	99.11	0.72	0.17

Apparatus. A microcatalytic reactor was built by using two Perkin-Elmer chromatography units. A Shell-Perkin-Elmer Sorptometer was used to provide a gas-mixing manifold and the facilities for surface area measurements. The principal modifications consisted of connecting the injection valve upstream from the first chamber of the detector and mounting a thermistor in place of the hot wire which is the usual detector provided with the Sorptometer.

The catalytic reactor was constructed by mounting an appropriate Pyrex glass catalyst holder provided with thermocouple wells in an FA-120 Hoskins furnace. This assembly was connected to the Sorptometer where an adsorbent is normally mounted for surface area measurements.

Effluent gas analysis was performed on a

Perkin-Elmer Vapor Fractometer (154C) with a precision Perkin-Elmer gas sampling valve for transfer of gas samples (25 ml) from the effluent stream from the microcatalytic reactor to the analytical column mounted in the Fractometer. A bubble flow meter and a Fischer-Porter Rotameter were mounted just beyond this sampling valve.

Gas analysis. The analytical conditions selected for the effluent gas analysis on the Vapor Fractometer were as follows: Hydrogen was analyzed on a coconut charcoal column with nitrogen elution gas. Oxygen was analyzed on a coconut charcoal column with helium elution gas.

Detection sensitivity for H_2 and O_2 using 3 ft $\times$ ¼ inch-ID columns, a flow rate of the elution gas of 25 ml/min, and a column temperature of 25°C was of the order of 25 ppm.

Test procedure. The test procedures used to evaluate the catalysts by oxidation with hydrogen in air are much the same as have been described by Emmett, Kokes, Tobin, and Hall (*2*, *3*).

The catalyst test system is shown schematically in Fig. 1. The catalyst bed in the Pyrex catalyst holder was 20 cm in length and about 1 cm in diameter. The entire catalyst zone fitted into a furnace well. Thermocouple wells were arranged down each side of the U-tube to each end of the catalyst bed. Copper-constantan thermocouples were used for the temperature measurements. Temperature gradients of the order of ±3° were usually observed between the ends of the catalyst bed. Over operating periods of several hours the variation in catalyst temperature was maintained within ±3°C. The catalyst tube and furnace were mounted in the normal adsorbent position on the Sorptometer so that the nitrogen area measurements could be made without remounting or disturbing the catalyst. The gas mixtures used in these experiments were either mixed on the manifold of the Sorptom-

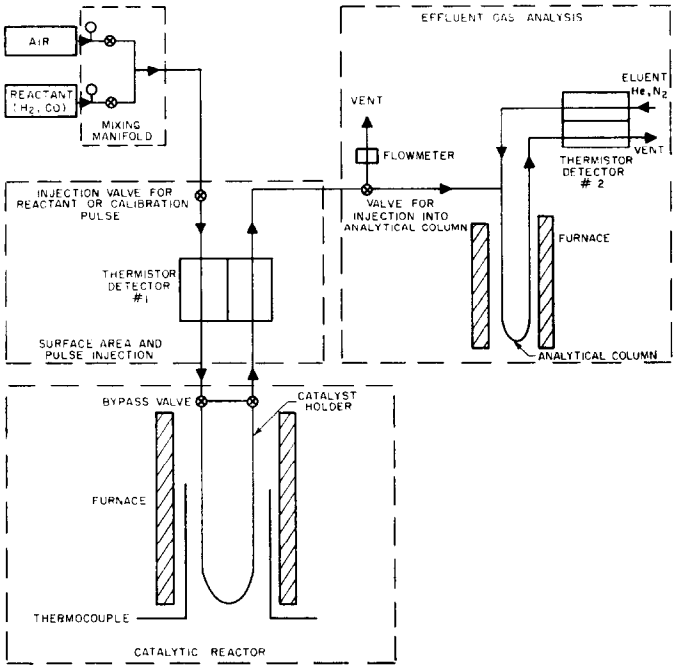

FIG. 1. Schematic diagram of microcatalytic reactor.

eter or were special analyzed mixtures purchased from the Matheson Company.

Pretreatment of the catalyst before each test run consisted of passing air at 44 ± 2 ml/min over the catalyst at 300°C for a period of 16 hr. The operating procedure and catalyst activation used with the N_2–H_2 gas mixtures were the same as used for the air–H_2 mixtures. Flow rates of 25 to 50 ml/min were used for the air–H_2 mixtures passed through the catalyst bed. The gas flow rates used for the N_2–H_2 mixtures were 15 to 25 ml/min. Mass spectrometer analysis of the N_2–H_2 mixture established the oxygen content to be less than 10 ppm.

Several experiments were performed on portions of this manganese dioxide at 410° ± 10°C to establish the magnitude of the readily available oxygen and the rates at which the oxygen can be removed from the oxide lattice (1) by thermal dissociation of the oxide eluted with an inert gas and (2) by depletive hydrogen oxidation by the oxide. These experiments were performed on unsupported manganese dioxide. The initial and final compositions of the oxides were determined by chemical analysis.

Results

Hydrogen Oxidation in Air

The dependence of the hydrogen oxidation rate on the hydrogen concentration for ~2000 to 60 000 ppm hydrogen in air over the temperature range of 25° to 300°C has been examined. Typical run data are given in Figs. 2 and 3. The run data in Fig. 2 are for relatively high hydrogen concentrations ranging from 38 000 to 52 000 ppm hydrogen in air. The data in Fig. 3 are for the low end of the hydrogen concentration range of the order of 2000 to 3000 ppm hydrogen in air. The attainment of an essentially constant effluent hydrogen concentration after run periods ranging from 60 to 100 min indicated a steady state condition for adsorption of oxygen and hydrogen, hydrogen oxidation, and desorption of the product water. The occurrence of the minima in the effluent hydrogen concentration, C_E, vs. time plots in Figs. 2 and 3 shows that upon first exposure of the catalyst to the hydrogen at temperatures of about 200°C and below some loss in oxidation capacity occurred. The catalyst was completely inactive in less than 100 min in the run at 32°C in Fig. 2. This loss in oxidation capacity is presumably due to water retention for at this low temperature retention of product H_2O can completely poison the catalyst for hydrogen

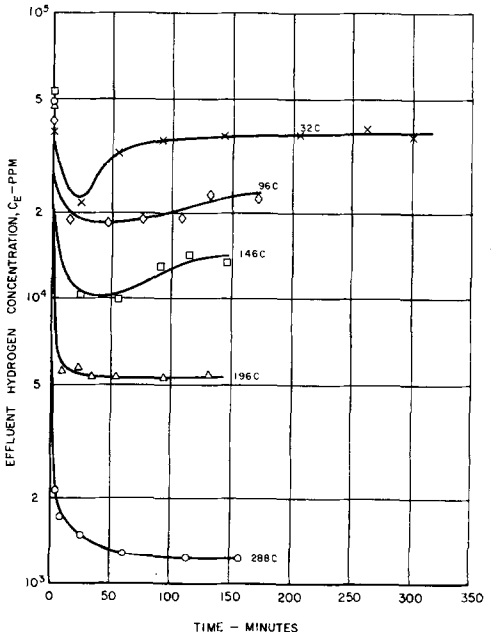

FIG. 2. Hydrogen oxidation in air (run data). Catalyst H-2-1-3.

oxidation. Representative run data for the range of hydrogen partial pressures and the temperature range studied are summarized in Table 2. Only at temperatures of 196°C and above are hydrogen oxidation efficiencies of 90% and better achieved. The oxidation rates, k, are reported in Table 2 as milliliters of H_2 NTP oxidized per gram of MnO_2 per minute.

In order to determine the specific oxidation rate constants, the following calculation was made for the kinetics of the hydrogen oxidation in an excess of air. The rate of hydrogen oxidation can be expressed by the equation

$$-dC/d\tau = k'C^n \qquad (1)$$

where C is the hydrogen concentration, τ is the transit time, n indicates the order of the

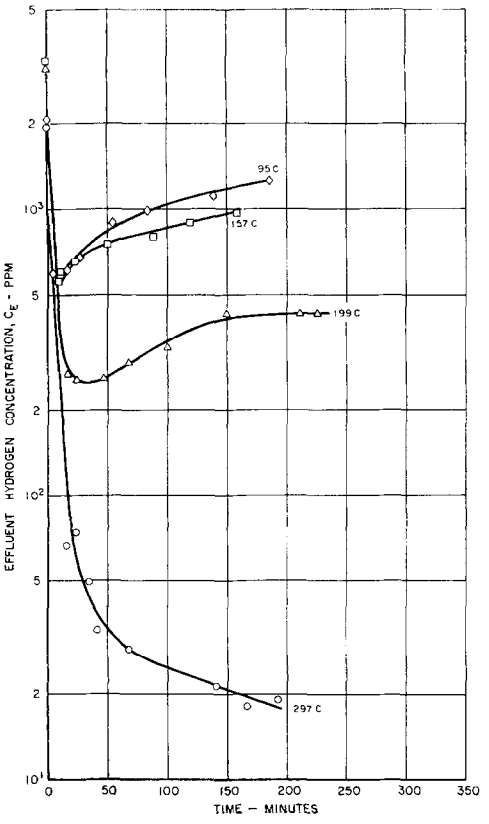

FIG. 3. Hydrogen oxidation in air (run data). Catalyst H-2-1-3.

reaction, and k' is the specific rate constant. Examination of the oxidation rates in Table 2 suggests a first order dependence with respect to hydrogen. In order to test this assumption, n was set equal to 1.0, and Eq. (1) was integrated to yield

$$k' = (2.303/\tau) \log_{10} (C_I/C_E) \qquad (2)$$

where C_I is the initial hydrogen concentration injected into the catalyst bed, C_E is the residual hydrogen concentration in the effluent gas stream leaving the catalyst bed, and τ is the transit time for a given increment of gas to pass through the catalyst bed for any given flow conditions. This transit time can be calculated from the flow rate for a given catalyst bed by the relation

$$\tau = \frac{(\pi r^2 L) - W/\rho}{V T_2/T_1} \qquad (3)$$

where r is the radius of the catalyst bed, L is the length of the catalyst bed, W is the weight of catalyst, ρ is the grain density of the catalyst, V is the measured volumetric flow rate at room temperature (T_1), and T_2 is the temperature of the catalyst for any given run condition.

Inasmuch as q_I, the total cumulative hydrogen injected into the catalyst bed after

TABLE 2

SUMMARY OF H_2 OXIDATION IN AIR RUN DATA[a]

Temp. (°C)	H_2 Injection C_I (ppm)	H_2 Effluent C_E (ppm)	Time (min) t_1	Time (min) t_2	H_2 oxidation efficiency $\frac{C_I - C_E}{C_I}$	H_2 oxidation rate, k $\left(\frac{\text{ml } H_2 \text{ NTP}}{\text{g } MnO_2 \text{ min}}\right)$ (Eq. 1)	Flow rate (ml/min)
95°	2060	669	26		0.675		44.1
		880		280	0.573	1.15	
96°	51 900	19 000	15		0.634		46.4
		22 900		168	0.559	36.9	
158°	3250	624	15		0.808		44.1
		987		155	0.696	2.65	
146°	52 200	10 150	25		0.806		42.4
		13 300		148	0.745	41.9	
199°	3250	265	15		0.918		44.5
		413		225	0.873	3.17	
196°	48 100	5660	18		0.882		42.4
		5230		130	0.891	44.1	
284°	5030	131	18		0.974		45.2
		86		132	0.983	5.44	
288°	49 100	1690	10		0.966		46.4
		1220		160	0.975	53.8	

[a] Catalyst H-2-1-3.

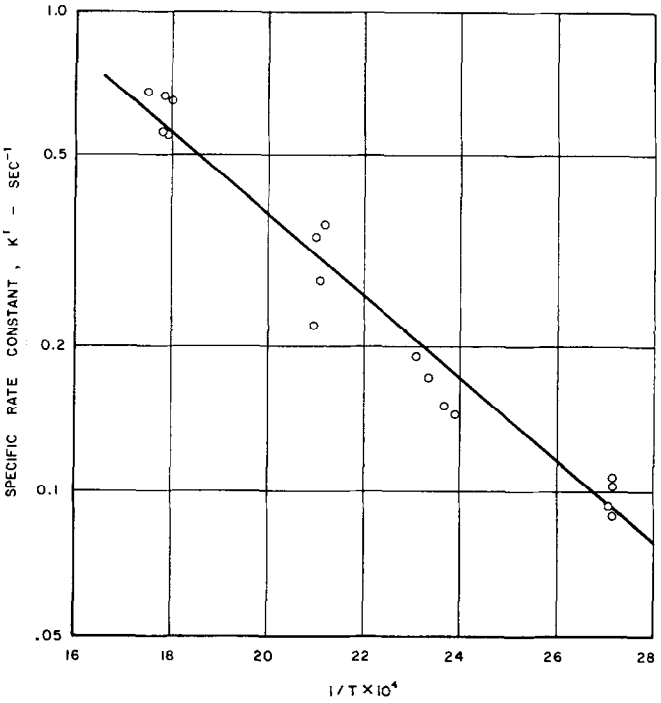

FIG. 4. Hydrogen oxidation in air (Arrhenius plot). Catalyst H-2-1-3.

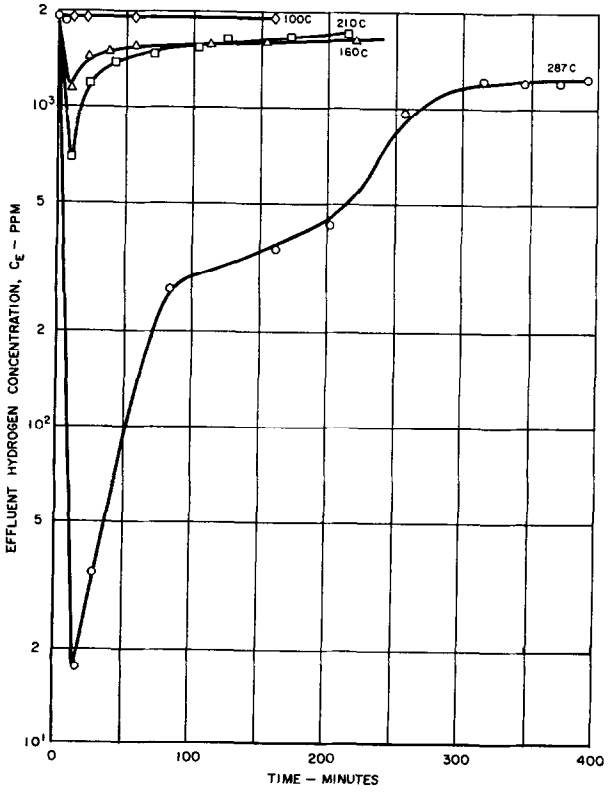

FIG. 5. Depletive oxidation of hydrogen (run data). Catalyst H-2-1-3.

any elapsed time t from the start of a given run is related to C_I by the expression $C_I = q_I/Vt$ and a similar expression $C_E = q_E/Vt$ related q_E, the total cumulative residual hydrogen in the effluent from the catalyst bed after any elapsed time t, Eq. (2) can also be plotted in the form

$$k' = (2.303/\tau) \log_{10} (q_I/q_E) \qquad (4)$$

The rate constants for a given temperature are reasonably constant for a wide range of C_I and it can be considered established that hydrogen oxidation over this catalyst in the presence of an excess of air over the temperature range 95° to 200°C is first order with respect to the hydrogen concentration.

The activation energy E for hydrogen oxidation in air was calculated to be 3.9 kgcal/mole (Fig. 4) from the Arrhenius equation (4)

$$k' = Ae^{-E/RT} \qquad (5)$$

This activation energy applies to the overall process of hydrogen adsorption, dissociation, and oxidation at the catalyst surface. The process can be visualized as a bimolecular reaction between dissociated hydrogen and an activated oxygen atom or hydroxyl group already present on the catalyst surface. The small magnitude of E indicates that hydrogen oxidation should proceed at a rapid rate at low temperature.

Depletive Oxidation of Hydrogen by Lattice Oxygen

The depletive oxidation of hydrogen by this manganese dioxide shows a first order reaction rate dependence upon the amount of manganese dioxide present. A series of oxidation runs made with a mixture of $N_2 + H_2$ in which the input hydrogen concentration was 1950 ppm over the temperature range from 25° to 300°C demonstrates this in Figs. 5 to 7. The run procedure and

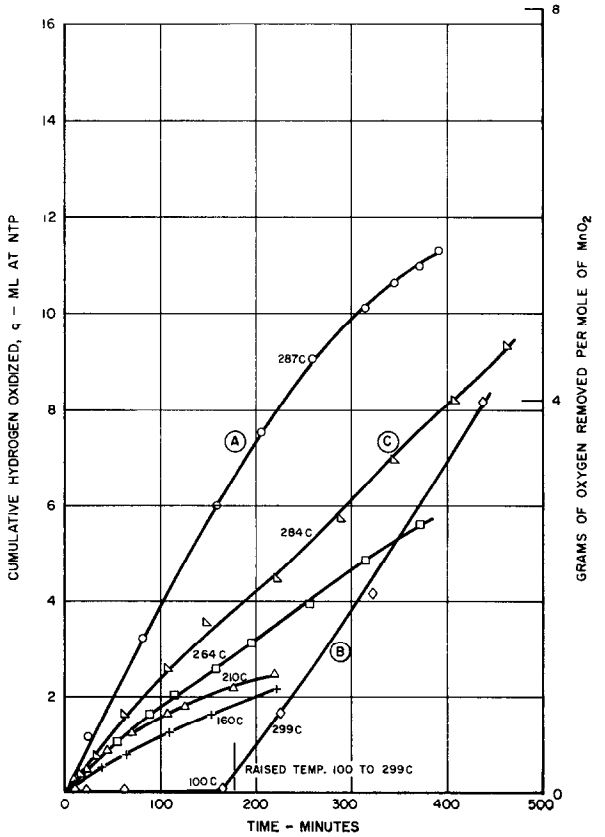

FIG. 6. Depletive oxidation of hydrogen (q vs. t). Catalyst H-2-1-3.

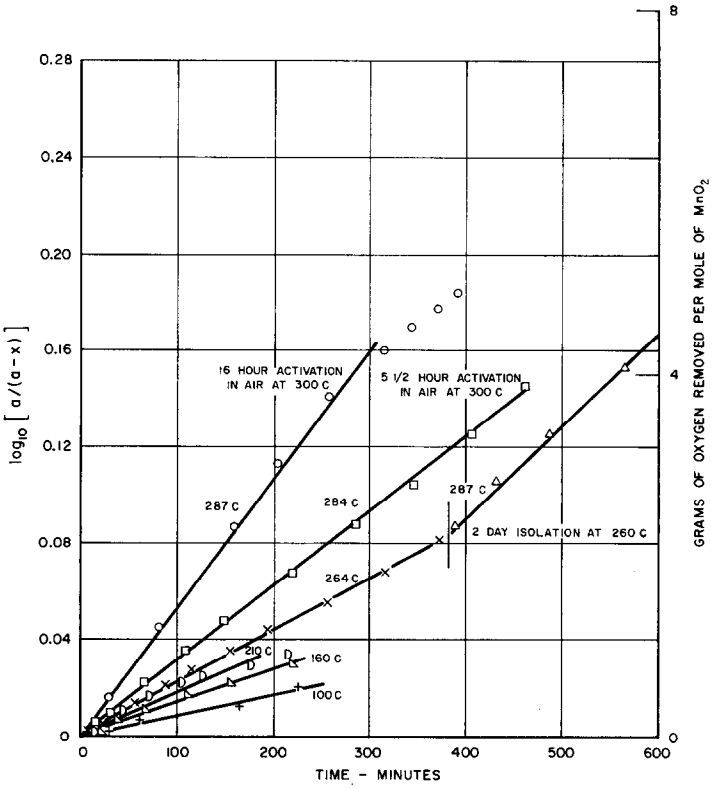

FIG. 7. Kinetics of depletive oxidation of hydrogen. Catalyst H-2-1-3.

effluent gas analysis procedures were in all respects the same as those used for the hydrogen oxidation in air runs. A plot of the cumulative hydrogen oxidation, q, versus time, t, is given in Fig. 6. A marked increase in the oxidation rate occurs at temperatures above 210°C. The appreciable differences in the initial portions of the three curves at 284°, 287°, and 299°C are due to the differences in sample history.

Curve A in Fig. 6 represents the first run made with the $N_2 + H_2$ mixture. Curve B represents data for a run made by raising the temperature to 299°C after a run period of 165 min at 100°C where negligible hydrogen oxidation had occurred. Curve C represents a run made on the catalyst upon conclusion of some seven hydrogen oxidation runs but with reactivation in air for $5\frac{1}{2}$ hr, instead of 16 hr, at 300°C. The initial portion of Curve A and the higher temperature portion of Curve B have essentially the same slope and, hence, the same hydrogen oxidation rate. The catalyst in both these instances was activated for 16 hr in air at 300°C. In the case of the short activation period (Curve C), the catalyst was oxygen deficient compared with its condition for all the other runs and this led to a lower initial hydrogen oxidation rate.

The marked increase in hydrogen oxidation rate above 200°C can be attributed in part to more rapid desorption of the product water and in part to increased mobility of the lattice oxygen. These data were found to fit a first order reaction rate plot,

$$2.303 \log_{10}[a/(a - x)] = k''t \qquad (6)$$

where a is the initial amount of manganese dioxide present in the catalyst and x is the oxygen removed by hydrogen oxidation at any time, t. The assumption is made for these calculations that the support Al_2O_3 provides no oxygen for the hydrogen oxidation.

These data are plotted in Fig. 7. The

curves are essentially straight lines for reaction times up to 400 min, except for the top curve of 287°C. For reaction times of 300 to 400 min at 287°C, the manganese dioxide was about one-half converted to Mn_2O_3 by the reaction,

$$2\,MnO_2 + H_2 \rightleftarrows Mn_2O_3 + H_2O \qquad (7)$$

A comparison of the heterogeneous hydrogen oxidation rates and the depletive oxidation of hydrogen rates at comparable hydrogen concentrations and run times for several temperatures is made in Table 3. In the depletive oxidation of hydrogen by the manganese dioxide diffusion of the lattice oxygen apparently controls the rate for only lattice oxygen is available. The depletive hydrogen oxidation rate at 100°C is only 1% to 2% of the heterogeneous hydrogen oxidation rate in air. The depletive hydrogen oxidation rates at 284° to 297°C range from one-half to one-third the observed heterogeneous hydrogen oxidation rates.

The activation energy for catalytic hydrogen oxidation in air was 3.9 kgcal/mole for the temperature range from 95° to 300°C. The activation energy for the depletive oxidation of hydrogen in the absence of gas-phase oxygen was calculated in a similar manner employing the oxidation rates given in Table 3 and the Arrhenius equation. This activation energy was 8.74 kgcal/mole for the temperature range 100° to 300°C. It can be concluded from a comparison of the oxidation rates and activation energies for the heterogeneous and depletive hydrogen oxidation processes that in the case of the heterogeneous process where gas-phase oxygen is readily available comparatively slight demand would be made upon the lattice oxygen at any depth from the catalyst surface.

Chemical Composition of Manganese Oxides

Based on the manganese analyses, this nonstoichiometric manganese dioxide preparation has a stoichiometry corresponding to $MnO_{1.95\pm0.02}$ compared with $MnO_{1.99}$ for reagent grade manganese dioxide. This nonstoichiometric preparation has a Mn^{2+} content which corresponds to 2% to 6% MnO. This indicates much more disorder within this oxide lattice than is characteristic of the high-purity reagent grade manganese dioxide

TABLE 3

A COMPARISON OF HETEROGENEOUS AND DEPLETIVE HYDROGEN OXIDATION RATES[a]

Temp. (°C)	H_2 (ppm) C_I	Oxygen source	Time (min) t_1	Time (min) t_2	H_2 (ppm) effluent C_E	H_2 oxidation rate at t $\left(\frac{\text{ml } H_2 \text{ NTP}}{\text{g } MnO_2 \text{ min}}\right)$	Flow rate (ml/min)
91°	2060	Air	26		669	1.52	44.1
				235	891	1.05	
100°	1950	Lattice	20		1918	0.021	30.4
				165	1928	0.011	
158°	3250	Air	25		670	2.80	44.1
				155	987	2.49	
160°	1950	Lattice	37		1474	0.29	24.7
				220	1622	0.20	
199°	3250	Air	24		248	3.27	44.5
				225	413	3.07	
210°	1950	Lattice	42		1375	0.40	24.8
				215	1699	0.17	
264°	1950	Lattice	20		1158	0.58	25.1
				195	1410	0.35	
297°	1970	Air	30		48	2.10	45.2
				190	19	2.14	
287°	1950	Lattice	28		35	1.03	21.9
				202	429	0.83	

[a] Catalyst H-2-1-3.

which contains 0.72% MnO. In reporting the chemical analyses, reduced Mn^{4+} is shown as manganese oxide since in solution Mn^{3+} is considered to be unstable and to have a transient existence unless bound in some chemical complex, whereas Mn^{2+} has stability in solution. In the next section on reaction mechanisms, Mn^{4+} is considered to be reduced to Mn^{3+} by reaction with hydrogen. Experimental confirmation is provided by the additional experiments described below.

A significant feature of the chemical analyses is that in the case of this nonstoichiometric manganese dioxide, initially, 8 to 13 wt % or about half a mole of combined water is present. The extremely small amount of other metal cations, even less than in the reagent grade manganese dioxide, precludes attributing this discrepancy to the presence of other metal oxides. The freshly prepared oxide prior to dehydration above 200°C can be represented by the formula MnO(OH).

Further information on this combined water and the availability of lattice oxygen was obtained from argon elution measurements at 400°C. Total weight loss for the active manganese dioxide was 15.0 ± 2 wt % compared with 0.13 ± 0.3 wt % for the reagent manganese dioxide. The water desorbed from these manganese dioxides was 8.8 ± 1.5 wt % for the active oxide and 0.4 ± 0.3 wt % for the reagent manganese dioxide, which is in good agreement with the water content based on the chemical analysis of these oxides (see Table 1). An estimate of the lattice oxygen desorbed was given by the difference between the total weight loss and the water recovered. This amounted to 6.2 ± 3.6 wt % for the nonstoichiometric manganese dioxide and <0.3 wt % for the reagent manganese dioxide.

The total oxygen removed from the active manganese dioxide based on the above elution data amounts to 0.17 moles of oxygen per mole of manganese dioxide. This represents total available oxygen atoms per cm^3 of the order of 1.2×10^{22}. In the case of the reagent manganese dioxide the above elution data indicate 10^{-4} moles of oxygen per mole of manganese dioxide or total available oxygen atoms per cm^3 of the order of 10^{20}. These chemical analyses are only accurate enough to indicate the defect nature of these nonstoichiometric oxides in a semiquantitative way. These data do provide, however, strong evidence of the increased availability of the oxygen in the catalytically active manganese dioxide and suggest that increased availability of the lattice oxygen leads to the creation of a large number of sites for either oxygen desorption or adsorption at comparatively low temperatures. In a heterogeneous catalytic reaction such as hydrogen oxidation in air only those sites at the gas–solid interface are involved. In the depletive oxidation of hydrogen or argon elution where the lattice oxygen diffuses to the gas–solid interface the "available" oxygen within the bulk of the oxide lattice is involved.

Several experiments at 410°C on the oxygen activation, helium elution, and depletive oxidation of hydrogen by this nonstoichiometric manganese dioxide led to the following results:

1. Activation of this nonstoichiometric manganese dioxide by exposure to an oxygen atmosphere for 3 days resulted in an oxide with the composition $MnO_{1.96}$. This oxide retained no more than 1.5% combined water.
2. The final compositions of two active oxide portions after 1350 and 1400 min of helium elution were $MnO_{1.53}$ and $MnO_{1.52}$.
3. Depletive oxidation of hydrogen by this nonstoichiometric manganese dioxide with an injection mixture of 1800 ppm hydrogen in nitrogen for a period of 2000 min produced an oxide with the final composition of $MnO_{1.5}$.

These experiments show that oxygen activation at 410°C does not quite build up the oxygen content of the active manganese dioxide to that of the reagent grade manganese dioxide which had a composition of $MnO_{1.99}$. These experiments also show that either helium elution or depletive oxidation of hydrogen by this active oxide for comparable periods of time leads to an oxide composition approximating Mn_2O_3.

An examination of the crystallographic structure of this especially active manganese

dioxide by X-ray diffraction analysis indicated a highly disordered structure and permitted a tentative identification with γ-MnO_2 (*5*). There are at least six common varieties of manganese dioxide: pyrolusite (β-MnO_2), cryptomelane (α-MnO_2), ramsdellite, psilomelane, γ-MnO_2, and δ-MnO_2. Crystallographic and electrochemical characteristics of γ-MnO_2 include (1) a sufficient homogeneity of crystallographic phase to permit reversible changes in oxidation state between MnO_2 and Mn_2O_3, (2) a high order of active oxygen as indicated by high activity as a depolarizer, (3) a highly defect lattice structure, and (4) a tendency to react with H^+ to form MnO(OH) (*5–9*).

Reaction Mechanism

The mechanisms for hydrogen and oxygen reactions with this manganese oxide are not completely understood, but the following suggestions are made concerning the general nature of these reactions, based on published studies made on other metal oxides. The surface reactions of the manganese oxide with oxygen can be visualized as follows ($\boxed{O^{2-}}$ indicates an oxygen ion vacancy):

$$O_2(g) \rightleftarrows O_2\ (Ads) \tag{8}$$

$$O_2\ (Ads) + (2)\ Mn^{3+} \rightleftarrows O_2^-\ (Ads) \text{ or } O\ (Ads) + O^-\ (Ads) \tag{9}$$

$$O^-\ (Ads) + Mn^{3+} \rightleftarrows O^{2-}\ (Ads) + Mn^{4+} \tag{10}$$

$$O^{2-}\ (Ads) + \boxed{O^{2-}}\ (lattice) \rightleftarrows O^{2-}\ (lattice) \tag{11}$$

The surface reactions of the manganese oxide with hydrogen can be visualized as follows:

$$H_2(g) \rightleftarrows 2H\ (Ads) \tag{12}$$

$$2H\ (Ads) + 2\ Mn^{4+} \rightleftarrows 2H^+\ (Ads) + 2\ Mn^{3+} \tag{13}$$

$$H^+\ (Ads) + O^{2-}\ (lattice) \rightleftarrows OH^-\ (lattice) \tag{14}$$

$$2H^+\ (Ads) + O^{2-}\ (lattice) \rightleftarrows H_2O + \boxed{O^{2-}}\ (lattice) \tag{15}$$

$$2H^+\ (Ads) + O^{2-}\ (Ads) \rightleftarrows H_2O \tag{16}$$

The net result of the several reactions of hydrogen and oxygen when both are present in the gas phase is that oxygen is adsorbed and made available in active form by oxidation of Mn^{3+} to Mn^{4+}, whereas the hydrogen is adsorbed and made available in reactive form by reduction of Mn^{4+} to Mn^{3+}.

For the conditions prevailing in the present experiments with low hydrogen concentration and an excess of oxygen present in the gas phase and with the temperature high enough that the manganese oxide lattice does not retain the product water, the net result of the reactions (8) through (16) leads to the manganese oxide acting as a true catalyst with an equivalence of the Mn^{3+} oxidized to the Mn^{4+} reduced. In the depletive oxidation of hydrogen over this manganese oxide, the possible reactions are limited to reactions (12) through (15) and the manganese dioxide is reduced to Mn_2O_3.

Acknowledgments

The author expresses appreciation to Dr. R. A. Arnoldi and Dr. G. L. M. Christopher for helpful discussions during the progress of this work, to Dr. G. Golden for the chemical analyses, and to the United Aircraft Corporation for permission to publish.

References

1. Brunauer, S., Emmett, P. H., and Teller, E., *J. Am. Chem. Soc.* **60,** 309 (1938).
2. Kokes, R. J., Tobin, H., Jr., and Emmett, P. H., *J. Am. Chem. Soc.* **77,** 5860 (1955).
3. Hall, W. K., and Emmett, P. H., *J. Am. Chem. Soc.* **79,** 2091 (1957).
4. Glasstone, S., Laidler, K. I., and Eyring, H. E., "The Theory of Rate Processes." McGraw-Hill, New York, 1941.
5. Tauber, J. A., "X-Ray Diffraction Key to the Manganese Oxide Minerals." E. J. Lavino and Co., Three Penn Center Plaza, Philadelphia, Pennsylvania, 1964.
6. Brenet, J. P., *Proc. Intern. Comm. Electrochem. Thermodyn. Kinet.* (*C.I., T.C.E.*), *8th Meeting,* p. 394 (Butterworths, London, 1956).
7. Brenet, J. P., Thirsk, H. R., and Tragardh, A. U., *Proc. Intern. Comm. Electrochem. Thermodyn. Kinet.* (*C.I., T.C.E.*), *9th Meeting,* p. 305 (Butterworths, London, 1957).
8. Ghosh, S., and Brenet, J. P., *Electrochim. Acta* **7,** 449 (1962).
9. Bode, von H., Schmier, A., and Berndt, D., *Z. Electrochem.* **66,** 586 (1962).